

Situational Awareness and Decision-Making for Distressed Aircraft

Israel Lopez¹, Nesrin Sarigul-Klijn¹

¹*Department of Mechanical & Aerospace Engineering, University of California, Davis, Davis, CA 95616, USA*
soylopez@ucdavis.edu
nsarigulklijn@ucdavis.edu

ABSTRACT

Situational awareness and decision-making are necessary to identify and select the optimal set of mutually non-exclusive hypothesis in order to maximize mission success by adapting system behavior accordingly. This paper presents a hierarchical and decentralized approach for integrated damage assessment and trajectory re-planning in aircraft with uncertainties in navigational decision-making. Aircraft navigation can be safely accomplished by properly addressing the following: decision-making, obstacle perception, aircraft state estimation, and aircraft control. When in-flight failures or damage occur resulting in an emergency, rapid and precise decision-making under imprecise information is required in order to regain and maintain control of the aircraft. In order to fly the pre-planned aircraft trajectory and complete safe landing, the uncertainties in system dynamics of the damaged aircraft need to be estimated and incorporated at the level of motion re-planning. The damaged aircraft is simulated via a simplified kinematic model. The different sources and perspectives of uncertainties in the damage assessment process and post-failure trajectory re-planning are presented. The decision-making process is developed via the Dempster-Shafer evidence theory. The objective of the trajectory re-planning is to arrive at a target position while maximizing the safety of the aircraft given uncertain conditions. Simulations are presented for an emergency motion planning and landing that takes into account aircraft dynamics, path complexity, distance to landing

site, runway characteristics, and subjective human decision.*

1. INTRODUCTION

In the past two decades, significant effort has been made towards the development of fault-detection-isolation-recovery (FDIR), and prognostics-health-management (PHM) sub-systems in order to increase safety and performance of aircraft systems (Nguyen *et al*, 2006; Jian and Kun, 2008). Discrete damage events, both on ground and in-flight, represent a threat to aircraft systems creating a distress event. Sources of discrete damage include hail impact, lightning strike, transport and handling damage, and foreign object impact. In addition, the high number of flight-cycles causes deteriorating permanent damage (Lopez *et al*, 2008). Under distress conditions, system dynamics may differ considerably from nominal, and the flight control performance may be significantly reduced. In such conditions, the distressed vehicle may not be capable of performing the mission goals which includes safe landing. Under distress conditions, pilot requires integration of obstacle awareness with intelligent decision-making, path planning and trajectory generation to achieve mission success. Decisions need be made during flight under uncertain conditions, such as limited information on failure conditions and cluttered environment. In this work, the framework for a distressed aircraft in-flight re-planning for optimal-length trajectories to safe landing is developed. The method presented here is designed to be used in conjunction with an integrated vehicle health monitoring (IVHM) and fault tolerant control (FTC) systems.

* Israel Lopez et al. This is an open-access article distributed under the terms of the Creative Commons Attribution 3.0 United States License, which permits unrestricted use, distribution, and reproduction in any medium, provided the original author and source are credited.

This paper develops a hierarchical approach for integrated decision-making, vehicle health monitoring, and motion planning under uncertain conditions. The objective is to achieve mission success, including safe landing, under the occurrence of distress events. The integrated decision, monitoring, and motion planning is demonstrated by means of 2D and 3D simulations of a simplified aircraft kinematics model.

2. INTEGRATED VEHICLE HEALTH MONITORING (IVHM)

The main objective of integrated vehicle health monitoring (IVHM) is to provide up-to-date vehicle health information via sensors, software and design. The information gathered is to be acted upon by decision-making mechanisms with intelligent reasoning to maximize a safe outcome probability. For a distressed aircraft, an IVHM system would provide valuable information to an adaptive or reconfigurable control system to achieve effective failure accommodation while updating flight performance regimes and determining the appropriate set of decisions followed by responses to complete mission to safe landing (Fahroo and Doma, 2004; Lopez *et al*, 2008). The generation of a flyable trajectory relies upon the knowledge of the vehicle's dynamic behavior and constraints. The dynamic characteristics are always approximate due to the uncertain knowledge, or the prediction methods used especially under vehicle faults, component failures and/or structural damage. The emergence and successful applications of PHM technologies over the last decade have given rise to proactive capabilities that can perform condition monitoring, detection of anomalies (faults), overall system state, predict system impacts, contingency management, and communication of contextual situational awareness to control mechanisms and system operators of human or autopilots. One of the areas of interest in implementing comprehensive IVHM functionality includes the detection and localization of impact events on structural and flight control surfaces.

In this paper, we demonstrate a proposed damage assessment approach by simulating an aircraft wing modeled as an isotropic aluminum cantilever beam of constant rectangular cross-section and an aspect ratio of 9.84. A recently proposed distance similarity matrix and combined dimensional reduction (D-R) technique, see (Lopez *et al*, 2008; Lopez *et al*, 2009) for more details, was applied to vibration data obtained from a base-excited cantilever beam. These techniques can assess the location and damage level resulting from impacts that may occur during flight. The beam was instrumented with 5-accelerometers at well-spaced discrete locations, and frequency response data was collected. Four different conditions were tested to simulate increasing structural damage where increasing

mass quantities were placed between two of the system sensors so as to simulate increasing loss of stiffness levels.

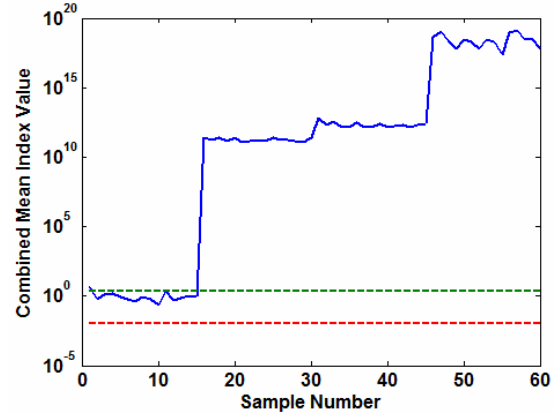


Figure 1. Combined dimensional reduction methods. NoMass: sample 1-15, Mass-1: sample 16-30, Mass-2: sample 31-45, Mass-3: sample 46-60.

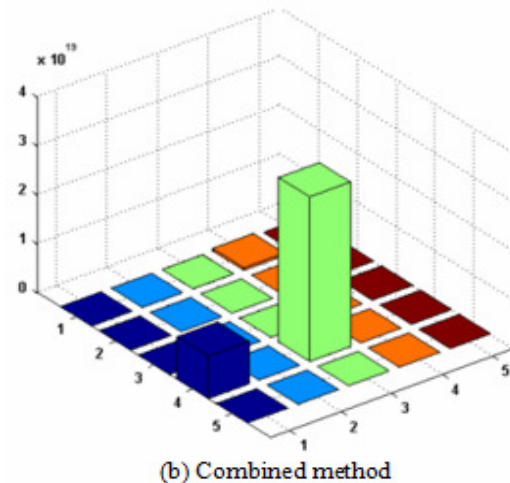
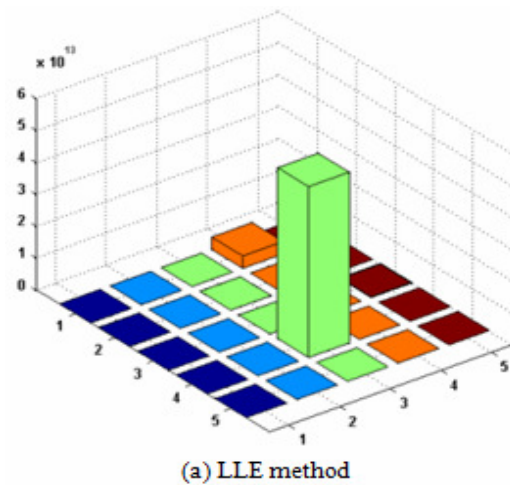


Figure 2. Localization results for Dataset-2, damage induced between sensors 3 and 4. Axis X and Y

represent sensor number, and Z axis represents the anomaly level.

Figure 1 shows the damage detection and tracking results obtained from vibration data. The upper and lower 3σ standard deviation limits of nominal structure are plotted. The mean index results indicate a difference among the multiple damaged datasets. The anomaly indicator index jumps both significantly and proportionally during the setup changes from an undamaged case to incremental levels of damage. The results of the distance similarity mean index in combination with the combined D-R technique demonstrate that not only can abrupt change detection can be achieved, but tracking of change progression can be performed, which would be very applicable to damage assessment of time-varying structures, such as deteriorating battle damage. Figure 2 shows the damage localization obtained from the vibration experiment when the induced damage was set between sensors 3 and 4. The damage localization results of two data-driven methods, local linear embedding (LLE) and a combined method proposed in (Lopez *et al.*, 2009). Both methods clearly indicate that large anomalies exist in relation to sensor 3 and 4. As previously stated, the experimental setup is representative of a damaged aircraft wing. By exploiting the vibrational characteristics of the cantilever wing-like structure, damage detection and localization was achieved by data-driven methods.

The information generated from these sub-systems can be integrated in-flight in response to vehicle damage and/or failure using updated dynamic constraints that reflect reduced vehicle maneuverability allowing for re-planning and re-shaping of the projected trajectory. For a nearly level steady coordinated turn and small-climb-angle approximation, the turn radius can be expressed in terms of load factor, n , and airspeed, V , as $R = V^2 / g\sqrt{n^2 - 1}$, where g is the gravitational acceleration. The load factor is an important parameter for all aircraft maneuvers involving curved flight. In damage events, significant portions of the aircraft's wing surface may be lost and would result in significant loss of lift and asymmetric mass properties. These combined changes would manifest in unstable and anomalous flight conditions. In addition, load carrying capacity of damaged aircraft would be reduced, which can result in further damage to critical lifting surfaces. (Nguyen *et al.*, 2006) and (Sarigul-Klijn *et al.*, 2008) simulated damaged aircraft flight dynamics, derived stability derivatives, and demonstrated that damaged wing results in significant reduction of lift coefficient, which minimizes the turning radius capability, reduction in lift and pitch moment causing an inability to hold attitude and flight

path angle, among other flight envelope complications. According to the results of Fig. 2, in the wing-like beam experiment, we studied and were able to detect three levels of damage. According to their degree of damage, fuzzy labels were assigned to the undamaged state and the three damage levels as shown in Fig. 4 and Table 1. The figure shows one membership function with four linguistic variables used from which a minimum turning radius is given, R_{\min} . The fuzzy labels are then sent to the inference engine. Based on the rule base, the inference engine digests the damage fuzzy labels and reaches a decision. For example, given a two-airport landing scenario, if damage is severe, then decision would indicate to land at closest airport since decreasing safe landing probability is inversely proportional to decreased time-in-flight after severe damage has been indicated. The types of failures addressed in this work are not necessarily found using derived stability derivatives or parameter state estimation. The approach here is to use a Dempster-Shafer (Shafer, 1976) inference system to make decisions based on the sampled diagnostic monitoring readings and a rule base. Diagnostic information is inputted to the expert system as a defined "degree of damage" to which the damage detected belongs to.

Table 1. Fuzzy Linguistic Variables

Linguistic Variable	Definition	R_{\min}
ND	No Damage	1
LD	Low Damage	2
MD	Moderate Damage	3
SD	Severe Damage	4

3. TRAJECTORY GENERATION

In this section, we present the distressed vehicle guidance problem. We assume that we have perfect knowledge of the terrain. The vehicle guidance problem is shown in Figure 3(a), where the vehicle's k -th position is given by $(x_k, y_k, z_k, \theta_k, \varphi_k)$. For the initial path planning, we will assume that the vehicle can move according to a heading angle φ , flight path angle θ and a distance β . The vehicle guidance problem, where the vehicle's $(k+1)$ position is given

$$\begin{bmatrix} x_{k+1} \\ y_{k+1} \\ z_{k+1} \\ \varphi_{k+1} \\ \theta_{k+1} \end{bmatrix} = \begin{bmatrix} x_k \\ y_k \\ z_k \\ \varphi_k \\ \theta_k \end{bmatrix} + \begin{bmatrix} \beta \cos(\varphi) \sin(\theta) \\ \beta \sin(\varphi) \cos(\theta) \\ \beta \cos(\theta) \\ \dot{\varphi}_{k+1} \Delta t \\ \dot{\theta}_{k+1} \Delta t \end{bmatrix} + \begin{bmatrix} \Delta_\beta \cos(\Delta_\varphi) \sin(\Delta_\theta) \\ \Delta_\beta \sin(\Delta_\varphi) \cos(\Delta_\theta) \\ \Delta_\beta \cos(\Delta_\theta) \\ \Delta_\varphi \\ \Delta_\theta \end{bmatrix} \quad (1)$$

where z is the height variable, x and y are the ground-tracking position variables.

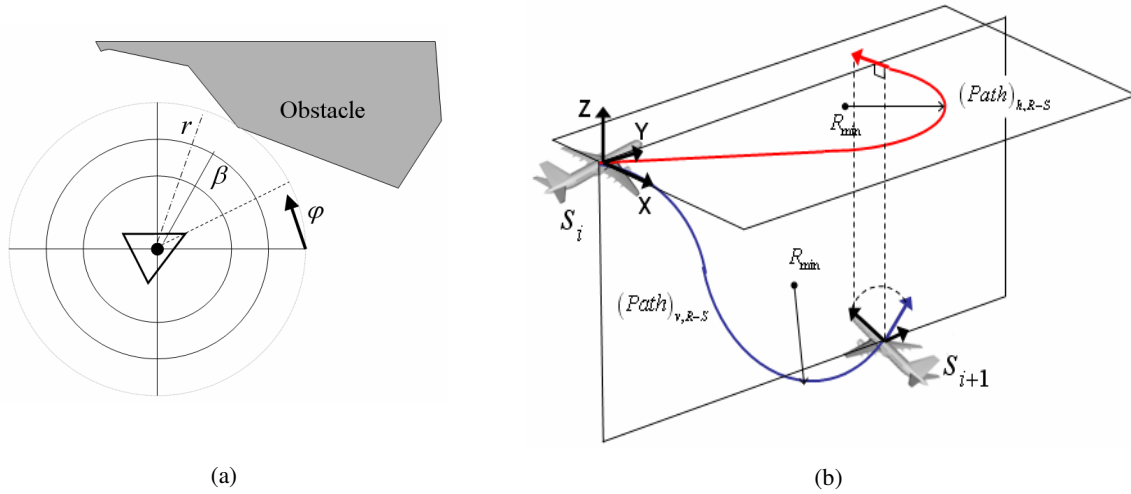


Figure 3. (a) Vehicle guidance problem; (b) 2D Reeds-Shepp curves integrated to obtain 3D path; adapted from (Hwangbo *et al*, 2007).

The sum of the first two terms represents the desired position, and the third term represents path uncertainty term due to inability of vehicle in achieving desired position. The uncertainty components $\Delta_\phi, \Delta_\theta, \Delta_\beta$ are distributed accordingly to some assumed known probability density function. The more uncertainty exists in the aircraft's performance, the larger these parameters are, which would be the case given the occurrence of a distressed event. The path planning is formulated as a steepest descent problem optimization, where it is assumed that the goal location (safest landing site), is the minimum point of the dimensional domain (Passino, 2005). Goal function is given by

$$J_g(x, y) = \left[[x, y]^T - [x_g, y_g]^T \right]^T \left[[x, y]^T - [x_g, y_g]^T \right] \quad (2)$$

where (x_g, y_g) is the desired final goal position.

In order to represent the obstacles, we use multiple Gaussian functions to generate a potential field or surface as given by

$$J_o(x, y) = \max \begin{pmatrix} m_{o,1} \left((x - x_{o,1})^2 + (y - y_{o,1})^2 \right) \\ m_{o,2} \left((x - x_{o,2})^2 + (y - y_{o,2})^2 \right) \\ \vdots \\ m_{o,n} \left((x - x_{o,n})^2 + (y - y_{o,n})^2 \right) \end{pmatrix} \quad (3)$$

where $m_{o,n}$ is a shape parameter, and $(x_{o,n}, y_{o,n})$ is the center location of n^{th} obstacle.

The objective function is chosen to be a weighted sum for a 2-airport scenario is given by

$$J(x, y) = w_{g,1} J_{g,1}(x, y) + w_{g,2} J_{g,2}(x, y) + w_o J_o(x, y) \quad (4)$$

where $w_{g,n}$ is a scale factor for each goal function, which determines preferred final goal, and w_o is a scale factor used to determine the risk level with respect to obstacle avoidance. The weights specify the relative importance of achieving obstacle avoidance and reaching the desired goal. The choice of these weights is rather important since it will affect the shape of trajectory and avoid obstacles. The following section will describe the analysis done via Dempster-Shafer (D-S) evidence theory to generate such weights. At each position (x_k, y_k) , the objective function J is computed at N_s values (x_k^i, y_k^i) , $i = 1, 2, \dots, N_s$, regularly spaced on a circle of radius r around the k -th vehicle position, by finding

$$J(x_k^*, y_k^*) \leq J(x_k^i, y_k^i), \quad i = 1, 2, \dots, N_s \quad (5)$$

which provides direction θ_k for vehicle's movement.

The path generated using the steepest descent method is piecewise linear and not suitable for an aircraft with kinematics and dynamic constraints. To smoothly connect this piecewise path, a cubic Bezier curve smoothing method is utilized, for further details see (Sarfranz and Khan, 2002). After determining the control points (fixes in this case), Bezier curves can be fitted to path generated which will result in a smooth path using Bezier interpolation. As an input, the maximum allowed square distance error between fitted path and smooth Bezier path has is given.

3.1 Length-Optimal Trajectory Generation

In this section, we study the problem of determining a length-optimal trajectory from a specified initial

configuration to a specified final configuration while considering the non-holonomic constraint and a limited turning radius of an air-vehicle in a ground track setup. The length-optimal path, proportional to shortest time types, is based on Reeds and Shepp (R-S) vehicle that can move forward and backward at a constant velocity. Subsequently, the sufficient family of the optimal trajectories can be obtained by combining the Pontryagin's Minimum Principle (PMP) with Lie algebras. The optimal trajectory presented in this paper is based on the work by (Wang *et al*, 2008) which used geometric local reasoning for achieving the sufficient family by PMP and a global reasoning for eliminating non-optimal trajectories within the sufficient family.

The kinematic model of the vehicle described in Eq. (1) can be represented as

$$\dot{q} = uf(q) + vg(q) \quad (6)$$

where $q = (x, y, \theta)$, $f(q) = (\cos(\theta), \sin(\theta), 0)^T$, $g(q) = (0, 0, 1)^T$, u and v describe, respectively, the linear and angular velocities of the vehicle.

The time-optimal trajectories of the vehicle and the path curves are based on a convexified Reeds-Shepp model. The notations of the base curves for the trajectory turning directions are described by the letters L, R, and S, respectively, left ($v=1$), right ($v=-1$) and straight ($v=0$). The + or - indicates that the motion is forward ($u=1$) or backward ($u=-1$). We want to find an admissible control (u, v) which, subject to Eq. (8), minimizes the total travel time. First, the adjoint vector, β , is introduced and we define

$$\gamma(t) = \langle \beta(t), f(q) \rangle, \quad \psi(t) = \langle \beta(t), g(q) \rangle \quad (7)$$

where $\gamma(t)$ and $\psi(t)$ are called the u -switching function and v -switching function, respectively. The Hamiltonian function, H , is expressed as (Chitsaz and LaValle, 2007)

$$H = \langle \beta, f(q)u + g(q)v \rangle = \gamma(t)u(t) + \psi(t)v(t) \quad (8)$$

From PMP, let the optimal control obtained be $(u^*(t), v^*(t))$ and $q^*(t)$ the corresponding state trajectory. Now, let $\beta(t)$ be a nontrivial solution to the adjoint equation

$$\dot{\beta}(t) = -\nabla_q H = -\left[u \frac{\partial f}{\partial q} + v \frac{\partial g}{\partial q} \right]^T \beta(t) \quad (9)$$

Minimizing the Hamiltonian function, we get $u^*(t) = -\text{sign}(\gamma(t))$, $v^*(t) = -\text{sign}(\psi(t))$. By PMP, there is a constant β_0 such that $\beta_0 = |\gamma(t)| + |\psi(t)|$.

Let $h(q) = [g(q), f(q)]$ denote the Lie bracket of the

vector field g and f . Introducing $\chi(t) = \langle q(t), f(t) \rangle$, then we obtain

$$\begin{aligned} \dot{\chi}(t) &= v(t)\chi(t) \\ \dot{\psi}(t) &= -u(t)\chi(t) \\ \dot{\chi}(t) &= -v(t)\psi(t) \end{aligned} \quad (10)$$

According to the above geometric reasoning, any two configurations, i.e. waypoints, of the vehicle can be linked by a minimum-length trajectory that belongs to the sufficient family of trajectories with additional global reasoning. For additional details on the optimal trajectory properties and categories please refer to (Wang, 2008). The optimal trajectory work based on R-S curves is used to integrate the k waypoint configuration, (x_k, y_k, θ_k) , to the next $k+1$ waypoint, $(x_{k+1}, y_{k+1}, \theta_{k+1})$, of the modeled vehicle. The waypoints are selected from the smooth Bezier curve.

Reeds-Shepp curves are designed for ground tracking path computation. In order to apply Reeds-Shepp curves to 3D motion, the dimensionality needs to be adjusted. The 3D vehicle trajectory between two waypoints is decomposed onto two orthogonal planes, i.e. xy-plane and yz-plane; see Fig. 3(b). 2D Reeds-Shepp curves are computed from both planes with projected configurations.

4. DECISION-MAKING

Given the scenario of a damaged airplane, a pilot may include various aspects of relevant information whose mapping to context information can be extremely complicated or fuzzy. Our goal is to maximize the probability or possibility of safe landing in which the vehicle's sensory data is fused with the pilot's perception and reasoning process in terms of environmental conditions and airport selection. To properly represent a situation of unknown or subjective decisions, it is necessary to allow interval-based assessment functions for which the Dempster-Shafer (D-S) theory (Shafer, 1976) provides a representation scheme and reasoning mechanisms for this context. The basic entity in the D-S theory is a set of exclusive and exhaustive hypotheses about some problem domain. It is called the frame of discernment, denoted as Θ . The degree of belief in each hypothesis is represented by a real number in $[0, 1]$. The basic belief assignment (BBA) is a function $m: \Psi \rightarrow [0, 1]$, where Ψ is the set of all subsets of Θ , the power set of Θ is $\Psi = 2^\Theta$. The function m can be interpreted as distributing belief to each of element in Ψ , with the following criteria satisfied:

$$\sum_{A \in \Psi} m(A) = 1, \quad m(\emptyset) = 0 \quad (11)$$

In evidence theory, we do not assign any degree of belief to the empty proposition \emptyset and we ignore the possibility for an uncertain parameter to be allocated outside of the frame of discernment. Thus, the element A is assigned a basic belief number $m(A)$ describing the degree of belief that is committed exclusively to A . Note that a situation of total ignorance is characterized by $m(\Theta) = 1$. The total evidence that is attributed to A is the sum of all probability numbers assigned to A and its subsets

$$Bel(A) = \sum_{\forall E: E \subseteq A} m(E) \quad (12)$$

Given that we have n number of information sources affecting decision-making, then each information source S_i will contribute by assigning its beliefs over Θ . The assignment function of each source is denoted by m_i . Thus, according to the information source's observation, the probability that the safest airport is indicated by the evidence interval $[Bel_i(A), Pl_i(A)]$, which reduces to a single point in the case of Bayesian belief function (BBF). The lower bound of interval is the belief function, which amounts for all evidence E_k that supports the airport selection A

$$Bel_i(A) = \sum_{E_k \subseteq A} m_i(E_k) \quad (13)$$

The upper bound of the evidence interval is the plausibility function, which accounts for all the observations that do not rule out the selection of airport A

$$Pl_i(A) = 1 - Bel_i(\bar{A}) = 1 - \sum_{E_k \cap A \neq \emptyset} m_i(E_k) \quad (14)$$

Because of uncertainty, the degree of belief for selecting Airport A and the degree of belief for a negation of selecting airport A do not have to sum up to 1. Given two independent belief functions over the same frame of discernment, Dempster's rule gives a way for combining BBA structures

$$(m_i \oplus m_j)(A) = \frac{\sum_{E_k \cap E_{k'} = A} m_i(E_k) m_j(E_{k'})}{1 - \sum_{E_k \cap E_{k'} = \emptyset} m_i(E_k) m_j(E_{k'})} \quad (15)$$

The denominator of Eq. (16) is a conflict of information given by independent information sources. Dempster's rule disregards every contradiction by normalizing with the complementary degree of contradiction because it is designed to use consistent opinions from multiple sources as much as possible.

For n mass functions m_1, m_2, \dots, m_n , the combined mass function and measure of contradiction are given by

$$m(A) = (m_1 \oplus m_2 \oplus \dots \oplus m_n)(A) = \dots \quad (16)$$

$$\frac{1}{1-C} \sum_{\cap_{i=1}^n E_i = A} m_1(E_1) \cdot m_2(E_2) \cdots m_n(E_n)$$

$$C = \sum_{\cap_{i=1}^n E_i = \emptyset} m_1(E_1) \cdot m_2(E_2) \cdots m_n(E_n) > 0 \quad (17)$$

5. SIMULATIONS

The following types of information sources are defined: integrated vehicle health monitoring (m_1), relative airport geography (m_2), environment (m_3), airport's resources (m_4), runway conditions (m_5), path complexity (m_6), and external human decisions (m_7). For the simulations, it is assumed a low-small damage (LD) with minimum radius $R_{\min} = 2$ and that information becomes incrementally available at four sections of the trajectory. Under an emergency scenario, interpretation, integration and decision-making is made incrementally since not all information is available at once. Table 2 shows the basic belief assignments (BBAs) and trajectory sections for each BBA derived for the specific airport scenario of Figure 5. For this particular airport selection, we simulate the scenario where the initial airport choice, B, is gradually changed for an abort airport, A. The abort decision is a subjective decision which is often made in real-world situations when selection advantages are not clearly quantifiable.

Table 2. Basic belief assignment (BBA) for Dempster-Shafer evidence theory analysis.

Input	Trajectory Section	BBA	A	B
IVHM	I, II, III, IV	m1	0.4	0.6
Relative airport geography	II, III, IV	m2	0.4	0.6
Environment	III, IV	m3	0.2	0.8
Airport resources	III, IV	m4	0.6	0.4
Runway characteristics	IV	m5	0.6	0.4
Path complexity	IV	m6	0.5	0.5
Subjective: human decision	IV	m7	0.01	0.99
	Information	Definition, T =simulation length		
Section I	m1	$t: 0 \rightarrow 0.3T$		
Section II	m1,m2	$t: 0.3T \rightarrow 0.5T$		
Section III	m1-m4	$t: 0.5T \rightarrow 0.7T$		
Section IV	m1-m7	$t: 0.7T \rightarrow T$		

Figure 4 shows the aggregations obtained via a weighted Dempster's rule of the BBAs in Table 2. A weighted Dempster's rule was used due to the amount of conflict in the BBAs. Figures 4(a)-(d) represent multiple levels of information aggregation acknowledging that from the distress event occurrence, the information gathering it's done at incremental information levels. As such, all available information, m_1 to m_7 , is not taken into account until the last section of the trajectory. As complete information becomes available, the decision becomes clearer.

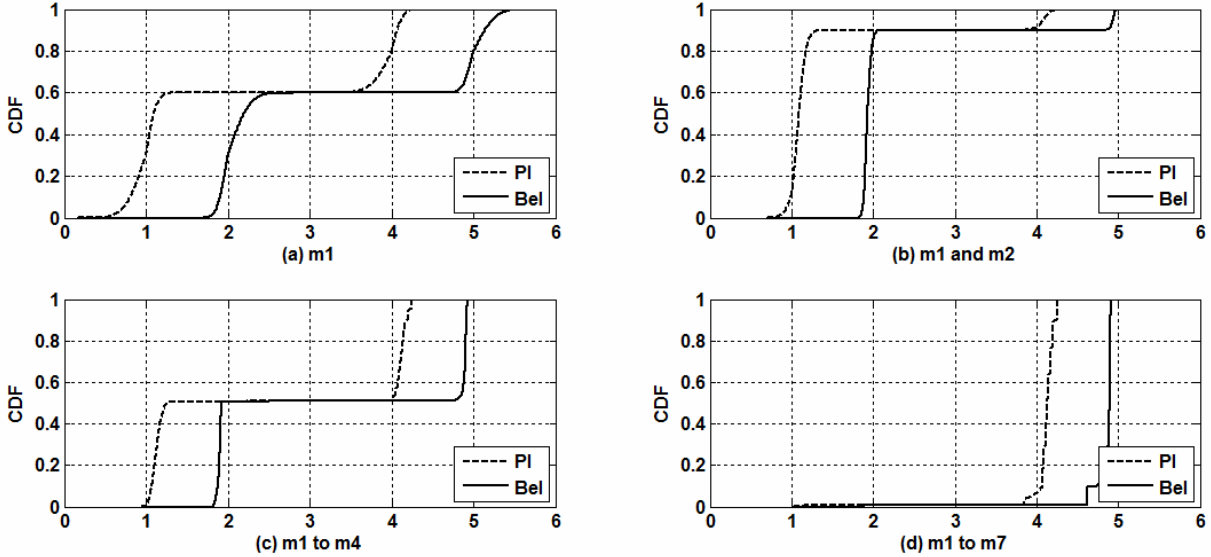


Figure 4. Cumulative distribution function (CDF) of combined mass functions. The interval for each airport are airport-B $\rightarrow [1,2]$, and airport-A $\rightarrow [4,5]$.

5.1 Case Study 1: Ground Tracking

For trajectory generation, we used a 2-airport selection scenario. The locations of the distress event and airports are set at $(0,0)_{distress}$, $(20,25)_A$ and $(28,10)_B$, respectively. Multiple obstacles (keepaway zones) are depicted by the high density contour lines around the distress event and near airport-A. The contour plot of the multiobjective function J shows the variances of the Gaussian obstacle functions and goal functions. The choice of the weights, obtained from the Dempster-Shafer analysis, will affect the shape of the trajectory that the vehicle will move toward its final goal position. Trajectory generation was performed at three different levels: (1) multiobjective function with uncertainty; (2) Bezier curve smoothing; and (3) optimal-length fixes generation. The multiobjective function is used as a guide for path heading. The smooth Bezier curve serves as a basis for waypoint selection, which is then utilized by the optimal-length trajectory. To simulate constraints generated from the damage event, the performance parameters are assumed to

The BBA aggregation is then used to generate the weights for the multiobjective function of Eq. (4), which is the basis for generating the distress event-to-airport trajectory. Fig. 4(a)-(b) shows a preference for airport B, which indicates the trajectory directed towards airport B. Fig. 4(d) shows that after more information is taken into account, the airport selection changes to airport-A, which becomes the landing airport for this simulation according to the BBA aggregation of all the information provided in Table 2.

be: turning radius $R_{min} = 2$, sensing radius $r = 3$, step size $\beta = 0.3$, location uncertainty $\Delta_\beta = N(0.1, 0.01)$, heading angle uncertainty with uniform distribution $-5^\circ \leq \Delta_\phi \leq 5^\circ$. Figure 5 shows the 2D trajectories generated using the multiobjective function, Bezier curve smoothing and the optimal-length waypoint approach. Due to the uncertainty, the path generated from the multiobjective path is irregular with sharp turns and changes in headings. By applying the Bezier curve smoothing, the sharp turns and erratic headings, such as sharp loops, are eliminated. The optimal-length trajectory by using Reeds-Shepp curves is shown with 10 waypoints, including initial and final position. Figure 5 shows that the proposed trajectory generation algorithm can avoid obstacles, and the 4-phase trajectory generation approach results in feasible trajectories under system constraints. Figure 6 shows multiple variations of the ground tracking

trajectory generation. The additional scenarios vary in obstacle number and locations, and also in goals locations. In all these scenarios, the trajectories are designed to start with an initial goal decision towards airport-B, and as new information becomes available at discrete times during the simulation, the evidence switches goal-selection towards airport-A. Fig. 6(b) demonstrates the capability of the path generation approach in avoiding collisions with obstacles. Fig. 6(c) and (d) were generated to demonstrate that sometimes incoming informational evidence might not be solely dependent in distance-to-goal. In these two cases, airport-A was obviously closer and easier to reach, but during emergency situations, proximity might not be the deciding criteria for choosing where to land the aircraft.

5.2 Case Study 2: 3D Trajectory

For the 3D trajectory generation, we used the airport selection scenario shown in Figure 7. The locations of the distress event and airports are set at $(1,1,12)_{distress}$, $(15,25,0)_A$ and $(26,15,0)_B$, respectively. Multiple obstacles are depicted by the high density contour lines around the distress event and near airport-A and -B. As in the 2D simulation, the weights for the multiobjective function were obtained using Dempster-Shafer analysis. To simulate constraints generated from the damage event, the performance parameters are the same as those used for the 2D case. The traveled distances obtained for each technique were 43.4 for the Path3 optimal-length trajectory, 44.15 for Path2 Bezier curve, and 45.83 for Path1 of the original potential function. It is important to note that Path3 minimum-length is optimal in between waypoints and not necessarily global minimum between initial point and landing point. Due to the uncertainty, the path generated from the multiobjective path is irregular with sharp turns and changes in headings. By applying the Bezier curve smoothing, the sharp turns and erratic headings are eliminated. Figure 7 shows that the proposed

trajectory generation algorithm can avoid obstacles in a 3D scenario. Fig. 7(c) shows the approximate paths to landing airports at each waypoint and were used to generate the BBA for each relative airport geography. By keeping track of the obstacle-free distance to all possible landing sites, a pilot or auto-pilot can weigh-in this information to decide if an abort site is achievable.

The use of Dempster-Shafer theory to integrate situational awareness information and provide proportional weights provides a systematic approach for performing decision-making; thus, airport selection and trajectory generation are performed on evidential reasoning. Because trajectory of aircraft cannot be adequately represented using line segments, the proposed framework uses Reeds-Shepp curves to produce continuous path lines described by set of waypoints chosen based on the recommended guidance information, which approximate strategies that a pilot would use given context information. The multi-criteria decision-making landing approach produced collision-free paths and successfully integrated context information to compute path decisions for each example. In ideal situations, decision makers are assumed to maximize or choose the best available choice, but maximizing requires thorough comparison of all possible alternatives, which in practice, may not always be possible and results in significant decision uncertainty. In the case of emergency landing scenarios, consideration of what makes a decision sequence satisfactory relies primarily on the safe outcome. Therefore, optimality in emergency decisions is not required, only decisions which result in a satisfactory safe outcome. Context informational data should be integrated to support human experts and non-experts in decision-making.

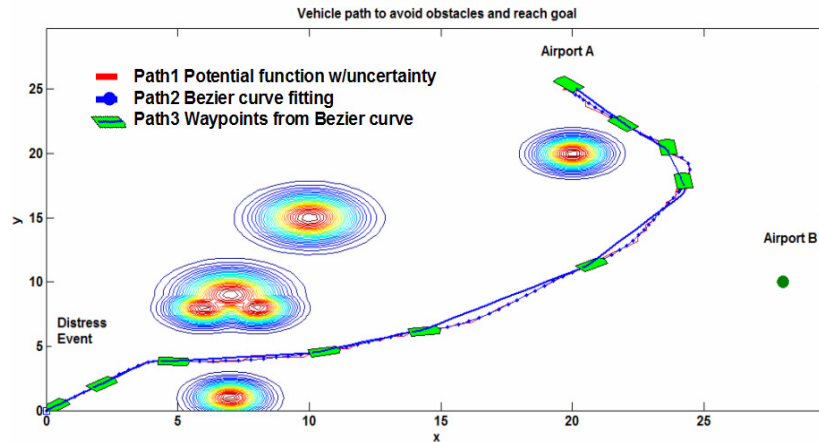


Figure 5. 2D paths for distressed aircraft under turn constraint with decision analysis.

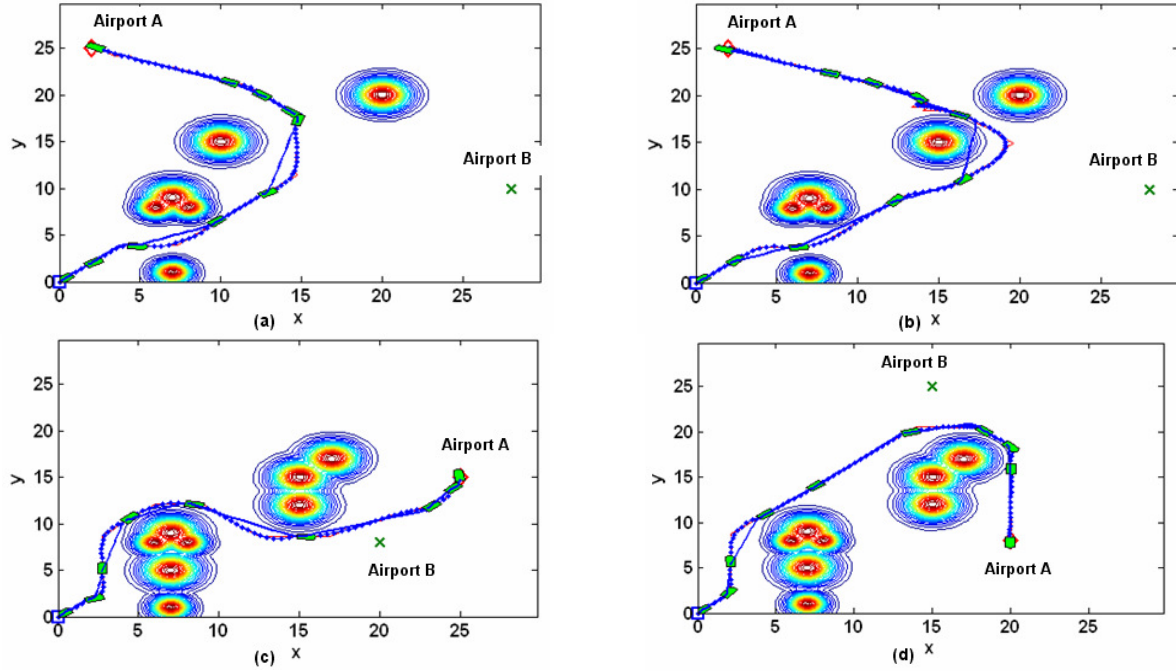


Figure 6. Multiple scenarios for 2D path generation.

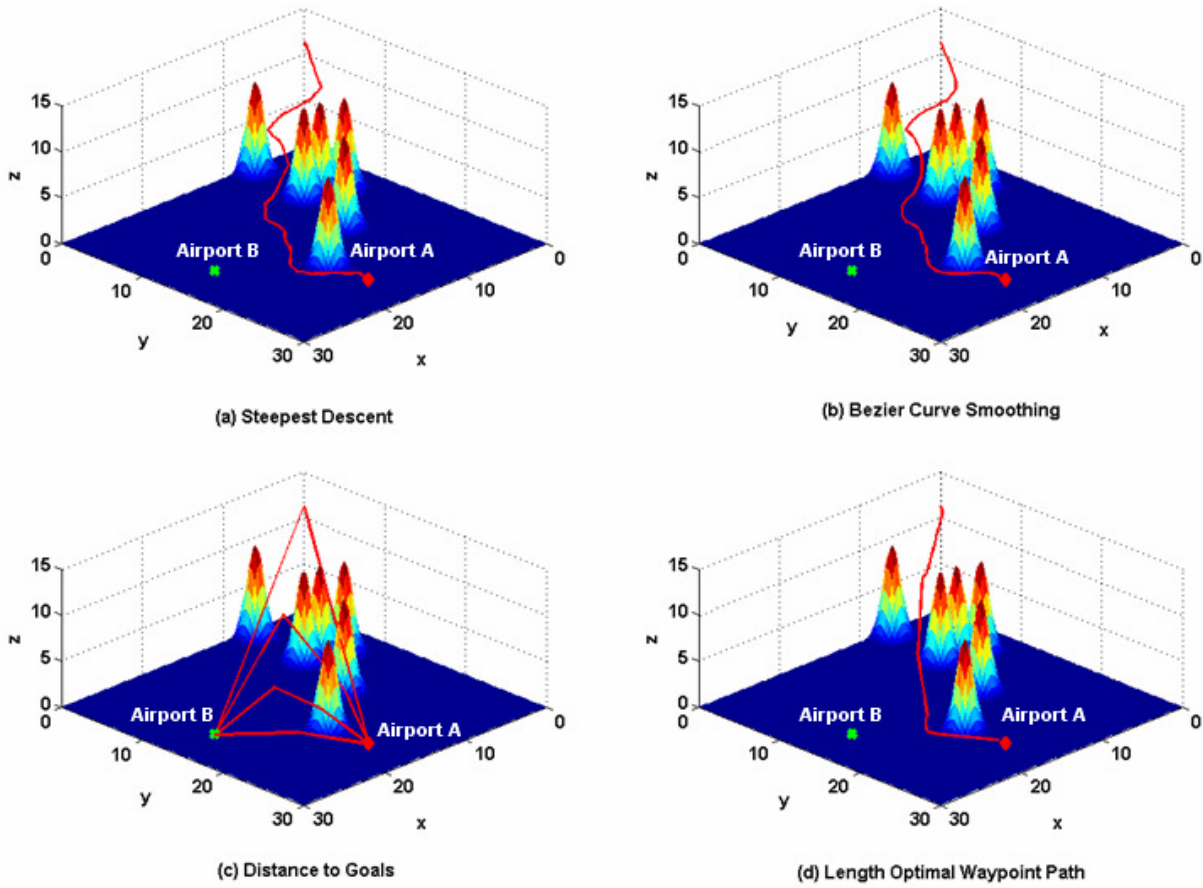


Figure 7. 3D paths for distressed aircraft under turn constraint with decision analysis.

6. CONCLUSION

This paper presents a hierarchical and decentralized approach for integrated damage assessment and motion planning in aircraft with uncertain navigational decision-making. The proposed approach for flight trajectory architecture developed in this research is an integration of IVHM with trajectory generation in particular when an abort decision is made for a secondary airport. Inclusion of vehicle health monitoring is important since damage or failures will likely be accompanied by reduced performance range and maneuverability. Under a in-flight distress condition, distance to the landing site becomes even more important. Hence, the optimal-length trajectory generation method developed here offers improvement by reducing the path length while increasing the probability of safe landing given the occurrence of an abort situation. Furthermore, the use of Dempster-Shafer evidence theory to integrate situational awareness information and provide proportional weights provides a systematic approach for performing decision-making. Preliminary simulation results have revealed a number of issues and challenges inherent to the application of expert systems in path planning and control. Future plans include further development and testing of the proposed approach on a high-fidelity simulator.

ACKNOWLEDGMENT

Research was funded in part by the Integrated Resilient Aircraft Control project under the NASA Cooperative Agreement NNX08AB96A.

REFERENCES

- (Chitsaz and LaValle, 2007) H. Chitsaz, S. M. LaValle, Time-optimal paths for a Dubins airplane, in *Decision and Control, 46th IEEE Conference on*, pp. 2379-2384, 2007.
- (Fahroo and Doma, 2004) F. Fahroo, D. Doma, A Direct Method for Approach and Landing Trajectory Reshaping with Failure Effect Estimation, in *AIAA Guidance, Navigation, and Control Conference and Exhibit*, Providence, Rhode Island, 2004.
- (Hwangbo *et al*, 2007) M. Hwangbo, J. Kuffner, T. Kanade, Efficient Two-phase 3D Motion Planning for Small Fixed-wing UAVs, in *Robotics and Automation, 2007 IEEE International Conference*, vol., no., pp.1035-1041, 10-14.
- (Jian and Kun, 2008) W. Jian, L. Kun, Multi-Sensor Data Fusion Based on Fault Detection and Feedback for Integrated Navigation Systems, in *Intelligent Information Technology Application Workshops International Symposium*, pp. 232-235, 2008.
- (Lopez and Sarigul-Klijn, 2008) I. Lopez, N. Sarigul-Klijn, System Identification and Damage Assessment of Deteriorating Hysteretic Structures, in *49th AIAA/ASME/ASCE/AHS/ASC Structures, Structural Dynamics, and Materials*, Chicago, IL, 2008.
- (Lopez and Sarigul-Klijn, 2009) I. Lopez, N. Sarigul-Klijn, Distance Similarity Matrix Using Ensemble of Dimensional Data Reduction Techniques: Vibration and Aeroacoustic case studies, in *Journal of Mechanical Systems and Signal Processing*, Vol. 23, Issue 7, pp. 2287-2300, 2009.
- (Nguyen *et al*, 2006) N. Nguyen, K. Krishnakumar, J. Kaneshige, P. Nespeca, Dynamics and Adaptive Control for Stability Recovery of Damaged Asymmetric Aircraft. in: *AIAA Guidance, Navigation, and Control Conference and Exhibit* Keystone, Colorado, 2006.
- (Passino, 2005) K. M. Passino, *Biomimicry for Optimization, Control, and Automation*: Springer, 2005.
- (Sarfraz and Khan, 2002) M. Sarfraz, M. N. Khan, Automatic Outline Capture of Arabic Fonts," *Information Sciences*, vol. 140, pp. 269-281, 2002.
- (Sarigul-Klijn *et al*, 2008) N. Sarigul-Klijn, P. Nespeca, T. Marchelli, M. Sarigul-Klijn, An Approach to Predict Flight Dynamics and Stability Derivatives of Distressed Aircraft. in *AIAA Atmospheric Flight Mechanics Conference and Exhibit*, Honolulu, HI, 2008.
- (Shafer, 1976) G. Shafer, *A Mathematical Theory of Evidence*. Princeton Univ. Press, 1976.
- (Wang *et al*, 2008) H. Wang, Y. Chen, P. Soueres, An Efficient Algorithm Involving the Canonical Switching Structure to Compute Minimum-length Trajectories for a Car, *Submitted to IEEE Transactions on Robotics*, 2008.